nature medicine

A quantitative basis for antiretroviral therapy for HIV-1 infection

Benjamin L Jilek[1], Melissa Zarr[2], Maame E Sampah[1], S Alireza Rabi[1], Cynthia K Bullen[1], Jun Lai[1], Lin Shen[1,2] & Robert F Siliciano[1–3]

Highly active antiretroviral therapy (HAART)[1–3] has dramatically decreased mortality from HIV-1 infection[4] and is a major achievement of modern medicine. However, there is no fundamental theory of HAART. Elegant models describe the dynamics of viral replication[3,5–9], but a metric for the antiviral activity of drug combinations relative to a target value needed for control of replication is lacking. Treatment guidelines[10,11] are based on empirical results of clinical trials in which other factors such as regimen tolerability also affect outcome. Why only certain drug combinations control viral replication remains unclear. Here we quantify the intrinsic antiviral activity of antiretroviral drug combinations. We show that most single antiretroviral drugs show previously unappreciated complex nonlinear pharmacodynamics that determine their inhibitory potential at clinical concentrations. We demonstrate that neither of the major theories for drug combinations accurately predicts the combined effects of multiple antiretrovirals. However, the combined effects can be understood with a new approach that considers the degree of independence of drug effects. This analysis allows a direct comparison of the inhibitory potential of different drug combinations under clinical concentrations, reconciles the results of clinical trials, defines a target level of inhibition associated with treatment success and provides a rational basis for treatment simplification and optimization.

To determine the antiviral activity of multidrug regimens, the inhibition produced by single drugs must be precisely quantified. Drug potency is commonly described using the concentration producing 50% inhibition in *in vitro* assays (IC_{50}). However, antiretroviral drugs are used at concentrations above the IC_{50}, and inhibition at clinical concentrations can only be determined if the shape or slope (m) of the dose-response curve is also known[12]. When dose-response curves are steep ($m > 1$), small changes in drug concentration (D) have large effects. Steep curves typically reflect cooperative binding to multivalent receptors[13]. However, antiretroviral drugs target enzymes that are univalent for the inhibitor. Thus, the slope parameter has been ignored even though it is a component of all fundamental pharmacodynamic equations[13–15] and models describing the combined effect of multiple drugs (reviewed in refs. 16,17). We previously showed that some antiretroviral drugs, notably protease inhibitors, have steep slopes[12]. This finding suggested unexpected complexity in the relationship between drug concentration and antiviral effect. To explore this relationship, we used a single-round infectivity assay[12,18], because complex factors such as growth and death of target cells distort m in multiround assays[19]. Infections were carried out in primary $CD4^+$ T lymphoblasts, the main target cells for HIV-1 *in vivo*[12]. The assay accounts for differences in protein binding, for the time required for intracellular phosphorylation of nucleoside reverse transcriptase inhibitors (NRTIs) and for individual variation in cellular uptake and metabolism of drugs (see Methods).

We also used a new method of analysis. Standard dose-response curves for antiviral drugs, which plot the fraction of infection events unaffected by drug (f_u) against log of drug concentration ($\log(D)$), obscure m, the importance of which is better illustrated in plots based on the median-effect equation[20] (equations (1) and (2)):

$$f_u = \frac{1}{1 + \left(\frac{D}{IC_{50}}\right)^m} \quad (1)$$

or

$$\log[(1 - f_u) / f_u] = m \log(D) - m \log(IC_{50}) \quad (2)$$

Equation (2) linearizes dose-response curves such that a logarithmic measure of inhibition, $\log[(1 - f_u) / f_u]$, increases linearly with $\log(D)$ (**Fig. 1a**). The slope of the line is m. With high inhibition ($f_u < 0.01$), $\log[(1 - f_u) / f_u]$ approximates $\log(1 / f_u)$, which is the instantaneous inhibitory potential (IIP), a useful and intuitive measure of antiviral activity[12]. IIP is the number of logs single-round infection events are reduced by a drug. Drugs with high m achieve much higher IIP than ones with the same IC_{50} but lower m (**Fig. 1a**).

The influence of m is apparent in HIV-1 infectivity assays[12,18] with different drugs. For the integrase strand transfer inhibitor (InSTI) raltegravir (RAL), curves generated with cells from different donors were

[1]Department of Medicine, Johns Hopkins University School of Medicine, Baltimore, Maryland, USA. [2]Department of Pharmacology and Molecular Sciences, Johns Hopkins University School of Medicine, Baltimore, Maryland, USA. [3]Howard Hughes Medical Institute, Johns Hopkins University School of Medicine, Baltimore, Maryland, USA. Correspondence should be addressed to R.F.S. (rsiliciano@jhmi.edu).

Received 17 October 2011; accepted 20 December 2011; published online 19 February 2012; doi:10.1038/nm.2649

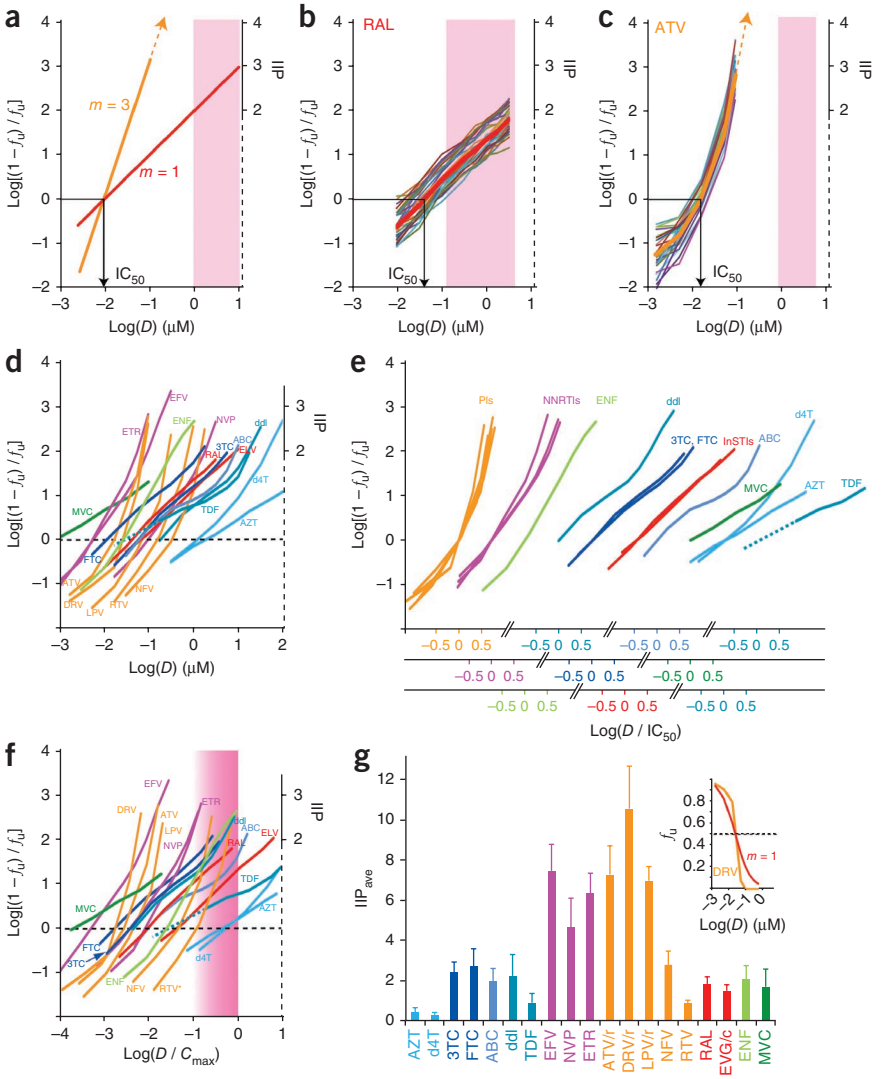

Figure 1 Determining inhibitory potential from complex dose-response curves of antiretroviral drugs. (**a**) Median-effect plots for hypothetical drugs with $m = 1$ or 3 and the same IC_{50}. Clinical concentrations 100–1,000 × IC_{50} are assumed (shaded pink). (**b**) Dose-response curves for RAL in primary $CD4^+$ T cells from 35 donors (thin lines) and mean curve (thick line). $m = 0.98 \pm 0.12$. The clinical concentration range is shaded in pink. (**c**) Dose-response curves for ATV. The clinical concentration range with standard dosing (once a day with RTV) is shaded in pink. (**d**) Mean dose-response curves for commonly used antiretroviral drugs. (**e**) Median-effect plots for classes of antiretroviral drugs. Plots from **d** are grouped by drug class or subclass, and, within each group, normalized by IC_{50}. The deoxyadenosine analogs ddI and TDF have very different slopes in the clinical range and are plotted separately. (**f**) Median-effect plots normalized by C_{max}. The shaded area represents the approximate clinical concentration range, the lower end of which is not precisely defined here because the relationship between C_{min} and C_{max} varies for different drugs. However, except for NRTIs, clinical concentrations generally remain within a log of C_{max}. Where appropriate here and in **g**, values reflect concentrations achieved with pharmacokinetic boosting. For RTV, the 100 mg dose is assumed. (**g**) Mean $IIP_{ave} \pm$ s.d. for commonly used antiretrovirals. Conventional dose-response curves (f_u versus log(D)) obscure the difference in the antiviral activity between a drug with a steep dose-response curve (DRV) and a hypothetical drug with the same IC_{50} and $m = 1$ (inset). /r, with low-dose RTV; ENF, enfuvirtide.

parallel and had slopes of ~1 (**Fig. 1b**). At the peak plasma concentration (C_{max}), RAL produces ~2 logs inhibition (IIP ≈ 2). Curves for the protease inhibitor atazanavir (ATV) are steeper and strikingly nonlinear (**Fig. 1c**). An upward inflection markedly increases inhibition for minor increases in D (**Supplementary Note 1**, **Supplementary Fig. 1** and **Supplementary Table 1**). Inhibition at clinical concentrations can only be estimated by extrapolation from the upper end of the observable range (**Fig. 1c**, **Supplementary Note 2** and **Supplementary Fig. 2**). At C_{max}, ATV produces ~8 logs of inhibition. Thus, infection of $>1 \times 10^8$ cells would be required to observe a single infection event.

Similar analyses showed that most antiretrovirals have complex, nonlinear median-effect plots (**Fig. 1d** and **Supplementary Table 1**). Different drugs showed highly significant differences in slope at clinical concentrations (m') (**Supplementary Table 2**). Grouping curves by drug class and normalizing by IC_{50} revealed that all protease inhibitors and non-nucleoside reverse transcriptase inhibitors (NNRTIs) have steep, upwardly inflected curves, with maximum slopes >3 and >2, respectively (**Fig. 1e** and **Supplementary Table 1**). These complex curves may reflect a unique form of intermolecular cooperativity[21]. Complex curves were observed for several other antiretrovirals (**Fig. 1e** and **Supplementary Note 3**). These results reveal previously unappreciated complexities in dose-response relationships for antiretroviral drugs that are crucial for understanding the effects of these drugs at clinical concentrations.

To demonstrate how these curves behave in the clinical range, we normalized concentrations by C_{max} (**Fig. 1f**). For the protease inhibitors ATV, darunavir (DRV) and lopinavir (LPV) and the NNRTI efavirenz (EFV), curves inflect upward at concentrations below the minimum plasma concentration (C_{min}), giving extraordinarily high IIP at clinical concentrations, consistent with clinical trial results[10,11]. For the protease inhibitor nelfinavir (NFV), the inflection occurs at $D > C_{min}$ (**Fig. 1f**), explaining its inferior clinical performance[22]. Because the protease inhibitor ritonavir (RTV) is used at low concentrations to 'boost' other protease inhibitors, its curve inflects at the top of the clinical range, providing little antiviral activity. Thus, understanding the complex shapes of dose-response curves at clinical concentrations is essential for assessing antiviral activity.

Pharmacokinetics are also important[12]. For drugs with high m, small decreases in D greatly reduce IIP. If the half-life is also short, IIP can fall dramatically during the dosing interval[12]. Therefore, we computed the average IIP over the dosing interval (IIP_{ave}) from the area under the IIP-versus-time curve to allow quantitative comparison of antiviral activity of different drugs at expected plasma concentrations (**Fig. 1g** and **Supplementary Tables 3** and **4**). We used equation (2) to model the dose-response relationship in the clinical concentration range, with parameters chosen to best represent the shape of the curve in that range (**Supplementary Table 1**). Notably, this calculation takes into account both the complex shapes of the dose-response curves revealed here and pharmacokinetic differences

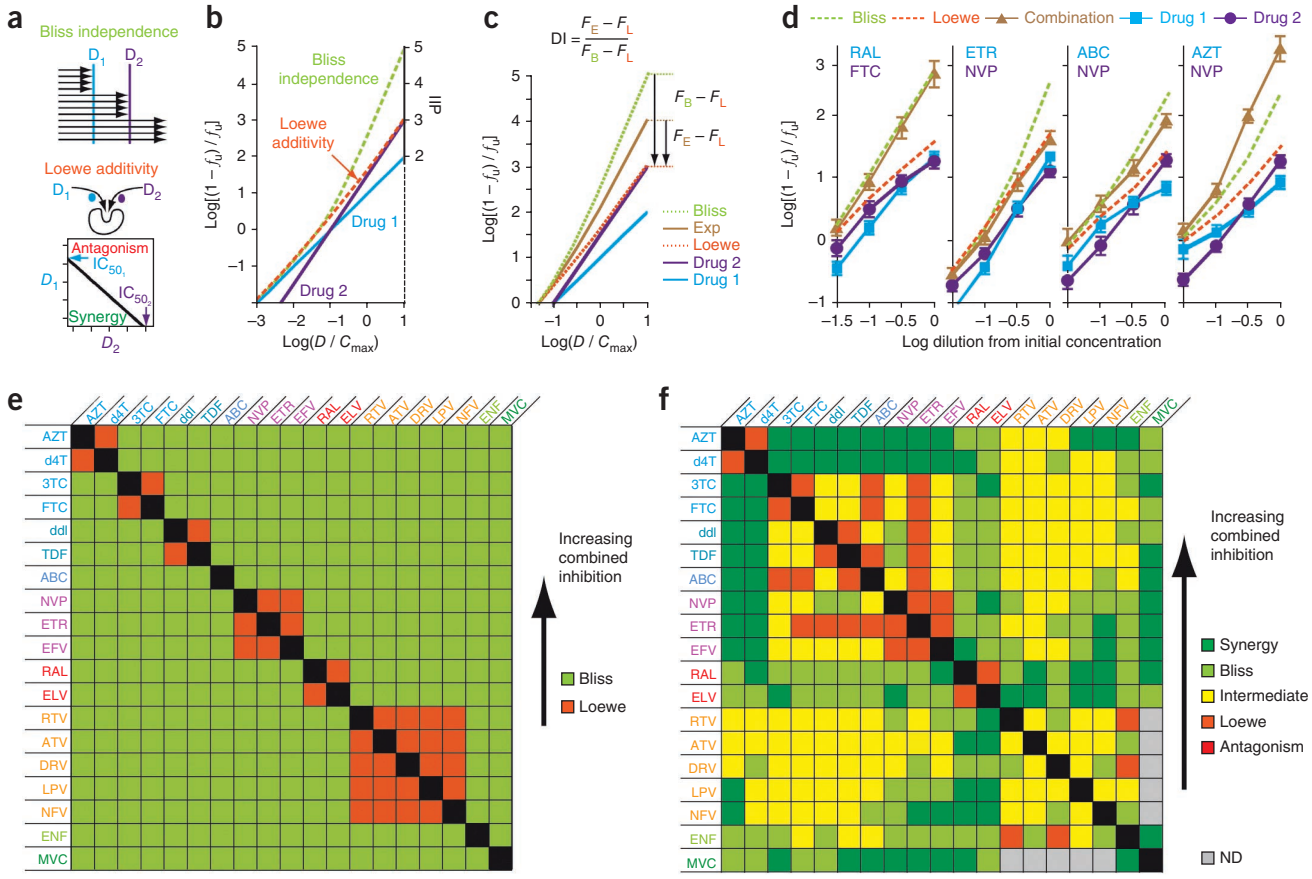

Figure 2 Combined effects. (**a**) Bliss independence and Loewe additivity models for hypothetical drugs D_1 and D_2. Loewe additivity is based on isobolograms depicting the concentrations of D_1 and D_2 needed to produce 50% inhibition (black line). Deviations to the left or right reflect synergy or antagonism, respectively, if Loewe additivity is the model for combined effects. (**b**) Median-effect plots for D_1 and D_2 alone (solid lines) and predictions of the combined effects of $D_1 + D_2$ by the Bliss and Loewe models (dashed lines). D_1 and D_2 have slopes of 1 and 1.5, respectively, and are diluted in constant ratio from $10 \times C_{max}$ which is assumed to be $10 \times IC_{50}$. (**c**) DI index for quantifying experimental (Exp) combined effects in relations to the models. (**d**) Representative combination experiments. Drugs were diluted at constant ratio from initial concentrations chosen to maximize the differences between the Bliss and Loewe predictions (see Methods). The figures show experimental measurements for single drugs and combinations (solid lines) and the predictions of the models (dashed lines). These examples illustrate characteristic patterns of Bliss independence (RAL-FTC), Loewe additivity (ETR-NVP), intermediate effect (ABC-NVP) and synergy (AZT-NVP). (**e**) Expected combination effects based on the binding-site criterion. (**f**) Observed combination effects categorized by DI values: synergy, DI > 1.2; Bliss, 0.8 < DI <1.2; intermediate, 0.2 < DI <0.8; Loewe, –0.2 < DI < 0.2, antagonism, DI < –0.2. Because of lower infection with R5-tropic pseudoviruses, protease inhibitor–MVC combinations could not be analyzed. Individual variation in the combined effect was substantial for some combinations (**Supplementary Fig. 4**). ND, not done.

between drugs. IIP_{ave} values in tissue sites that have different drug concentrations than plasma could be similarly estimated provided that the relevant pharmacokinetic data were available.

Overall, the results explain the established clinical value of NNRTIs and protease inhibitors[10,11]. Treatment guidelines have until recently recommended that all initial HAART regimens include an NNRTI or protease inhibitor[10,11]. Steep, upwardly inflected curves allow these drugs to achieve extremely high IIP_{ave}. We previously estimated that 1×10^6 infection events occur per viral generation in the average untreated patient, suggesting that $IIP_{ave} > 6$ would be required to immediately halt replication[23]. Only NNRTIs and protease inhibitors approach this level. The protease inhibitor DRV has the highest IIP_{ave}. Of note, protease inhibitors are the only class for which monotherapy has been successful[24–26]. Conventional dose-response curves obscure the marked differences in IIP observed here (**Fig. 1g**).

Some drugs with low IIP_{ave} such as RAL and the chemokine receptor antagonist maraviroc (MVC) are effective in combination therapy[27,28]. We hypothesized that these drugs might have favorable or synergistic interactions in combinations that compensate for low intrinsic IIP_{ave}. However, there is no metric for the antiviral activity of antiretroviral drug combinations. Two fundamental models describe the combined effects of multiple drugs[16,17] (**Fig. 2a**). Bliss independence[29] assumes independent action such that the combined effect (f_{u1+2}) is the product of the fractions unaffected by each drug (equation (3)):

$$f_{u1+2} = f_{u1} \times f_{u2} = \frac{1}{1 + \left(\frac{D_1}{IC_{50_1}}\right)^{m_1}} \times \frac{1}{1 + \left(\frac{D_2}{IC_{50_2}}\right)^{m_2}} \quad (3)$$

Loewe additivity[30] is based on isobolograms and assumes similar mechanisms or competition for the same binding site. For positive inhibitory slopes, Loewe additivity is described by equation (4):

$$1 = \frac{D_1}{IC_{50_1}\left(\frac{f_{u1+2}}{1 - f_{u1+2}}\right)^{-1/m_1}} + \frac{D_2}{IC_{50_2}\left(\frac{f_{u1+2}}{1 - f_{u1+2}}\right)^{-1/m_2}} \quad (4)$$

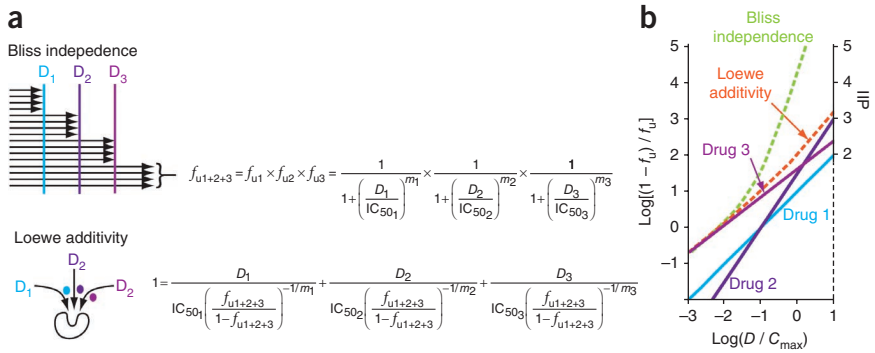

Figure 3 Estimating the inhibitory potential of triple combinations. (**a**) Expansion of the Bliss and Loewe models to three drugs. The three-drug Bliss formula is based on a simple extension of the idea that the fraction of viruses unaffected by the blocks imposed by three drugs acting at different steps in the life cycle (f_{u1+2+3}) is the product of the fraction unaffected by each drug. The Loewe formula is based on the idea the inhibitors act in a mutually exclusive way or compete for the same binding site as discussed by Chou[17]. It is derived from the general expression for an *n* drug combination with no synergy of antagonism as described in the **Supplementary Methods**. (**b**) Median-effect plots for hypothetical drugs D_1, D_2 and D_3 alone (solid lines) and predictions of the combined effects of $D_1 + D_2 + D_3$ by the Bliss and Loewe models (dashed lines). D_1, D_2 and D_3 are diluted in constant ratio from $10 \times C_{max}$ and assumed to have IC_{50} values of 0.1, 0.1 and $0.01 \times C_{max}$ and slopes 1, 1.5 and 0.8, respectively.

Bliss independence predicts higher inhibition than Loewe additivity, with upwardly inflected curves (**Fig. 2b**). Synergy and antagonism can only be defined relative to the combined effect predicted by a given model. Loewe additivity is generally chosen[16,17] despite the fact that, by simple binding-site competition criterion, Bliss independence should apply to many antiretroviral drug combinations, particularly those involving drugs acting at different steps in the life cycle. However, there has been no systematic evaluation of which model applies to antiretroviral drugs. Therefore, we analyzed 166 of 171 possible pairwise combinations of 19 commonly used antiretrovirals. Of note, we used conditions maximizing the difference in the levels of inhibition predicted by the two models (see Methods).

Experimental inhibition unambiguously fit one of the standard models for <60% of combinations (**Supplementary Fig. 3**). Intermediate inhibition was common and can be understood by considering NRTI-NNRTI interactions. Although these classes bind different sites on reverse transcriptase, they inhibit the same process and are not fully independent. Therefore, these combinations show inhibition below the Bliss prediction. Notably, the inhibition produced by a given combination showed a consistent relationship to predictions of the two models as drug concentrations increased (**Fig. 2c**). This suggests that combinations can be characterized on a spectrum defined by two states, independent inhibition (Bliss) and competitive binding (Loewe), with synergistic and antagonistic interactions at either extreme. To quantify degree of independence (DI), we developed a new index with combinations following Loewe additivity assigned DI=0 and combinations following Bliss independence assigned DI=1. The index is computed as:

$$DI = \frac{F_E - F_L}{F_B - F_L} \quad (5)$$

where F_E, F_L and F_B are logarithmic measures of inhibition, $\log[(1 - f_u) / f_u]$, for the experimental data and Loewe and Bliss predictions, respectively (**Fig. 2c**). This approach incorporates both classic models and maps inhibition on a median-effect plot in relation to the models.

Representative combination experiments are shown in **Figure 2d**. Expected results based on the competitive binding criterion are in **Figure 2e**. Experimental results, categorized by DI index, are in **Figure 2f** and **Supplementary Table 5**.

Some combinations targeting different steps in the life cycle followed Bliss independence and showed higher combined effects. This is illustrated by the InSTI-NRTI combination RAL-emtricitabine (FTC) (**Fig. 2d**, $R^2 = 0.99$ for Bliss) and was observed for combinations of InSTIs with drugs from all other classes (**Fig. 2f**). The excellent clinical performance of InSTI-based regimens[27] may reflect these favorable interactions. The chemokine receptor antagonist MVC also showed favorable interactions (**Fig. 2f**).

Drugs binding to the same site, such as the hydrophobic NNRTI pocket[31], should follow Loewe additivity. This is illustrated by the NNRTI-NNRTI combination etravirine (ETR)-nevirapine (NVP) (**Fig. 2d**, $R^2 = 0.99$ and 0.64 for Loewe and Bliss, respectively). Loewe additivity was observed for combinations of two NNRTIs, two InSTIs and two nucleoside analogs of the same base (zidovidine-stavudine (AZT-d4T), lamivudine (3TC)-FTC and didanosine-tenofovir (ddI-TDF)) (**Fig. 2f**). The AZT-d4T combination is considered antagonistic owing to effects at the level of phosphorylation[32] and suboptimal clinical responses[33]. However, in infectivity assays, this combination fits the Loewe prediction perfectly ($R^2 = 0.99$).

Another common pattern was a combined effect between the Bliss and Loewe predictions, reflecting some lack of independence. This is illustrated by the NRTI-NNRTI combination abacavir (ABC)-NVP (**Fig. 2d**). Intermediate effects were observed for many RTI–protease inhibitor combinations and some RTI-RTI and protease inhibitor–protease inhibitor combinations (**Fig. 2f**, **Supplementary Table 5** and **Supplementary Fig. 4**) As discussed above, lack of independence is expected for combinations of RTIs and, for protease inhibitor–RTI combinations and protease inhibitor–protease inhibitor combinations, may represent complex effects of incomplete maturation on downstream events in the life cycle[34–36]. Combined effects significantly greater than the Bliss prediction represent synergy and were observed for combinations of deoxythymidine analogs AZT or d4T with other RTIs (**Fig. 2d**, AZT-NVP and **Fig. 2f**) and for certain other combinations (**Fig. 2f**). Together, these results suggest that degree of independence of two drugs has a major impact on the combined effect.

IIP for triple combinations (IIP_{1+2+3}) can be estimated using three drug versions of the Bliss and Loewe models, with Bliss independence predicting higher combined effects (**Fig. 3**). Antagonism, defined as inhibition less than the Loewe prediction, was uncommon in pairwise analysis (**Fig. 2f**). Therefore, we assumed that the lower limit of IIP_{1+2+3} is the Loewe prediction. Similarly, since most two drug combinations showed inhibition less than or equal to the Bliss prediction, the upper limit of IIP_{1+2+3} is the Bliss prediction except for cases in which strong synergistic interactions dominate. Using these bounds, we determined the range of $IIP_{ave1+2+3}$ for all three

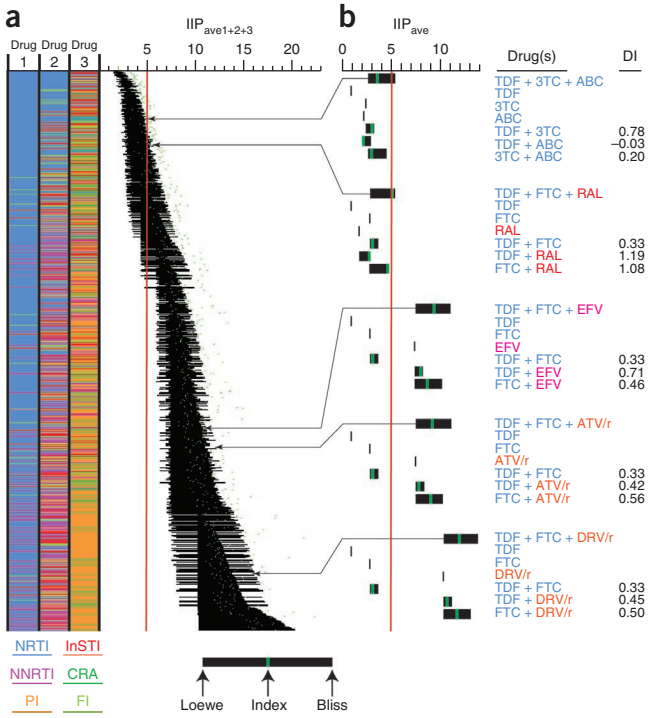

Figure 4 Inhibitory potential of three drug combinations. (**a**) Estimated $IIP_{ave1+2+3}$ for triple combinations of 19 commonly used antiretrovirals. Combinations are color-coded by drug class, excluding combinations with more than one drug from the NNRTI, protease inhibitor (PI) or InSTI classes or NRTI subclasses. CRA, chemokine receptor antagonist; FI, fusion inhibitor. The black bars represent the range of estimated $IIP_{ave1+2+3}$ values with the Loewe prediction at the left and the Bliss prediction at the right. Regimens are sorted based on the midpoint of the range. An estimate based on the weighted average of the three pairwise DI index values is shown as a green dot. $IIP_{ave1+2+3}$ values above the Loewe-Bliss range represent synergy, typically for regimens including thymidine analogs. The red line represents the minimum $IIP_{ave1+2+3}$ for a regimen achieving suppression of viremia in >80% of patients. (**b**) Inhibitory potential of selected three-drug combinations along with component single drugs and drug pairs. For combinations, inhibitory potential is shown as a range of $IIP_{ave1+2+3}$ values between the Loewe and Bliss predictions. For each component two drug combination, an estimate of IIP_{ave} based on experimentally determined DI index values is shown as a green bar. For three-drug combinations, green bars represent estimates based on a weighted average of pairwise DI index values. Values are shown for currently recommended initial HAART regimens[10,11] and, for purposes of comparison, a suboptimal TDF plus 3TC plus ABC regimen[38].

drug combinations of 19 commonly used antiretrovirals (**Fig. 4a** and **Supplementary Table 6**). Because the Bliss and Loewe predictions diverge with increasing D (**Figs. 2b** and **3b**), the ranges are broad. Predicted $IIP_{ave1+2+3}$ values for different regimens vary substantially. At the high end are regimens with two drugs whose dose-response curves inflect sharply upward at $D < C_{min}$ (for example, EFV plus DRV). At the low end are dual-NRTI regimens. To examine the relationship between $IIP_{ave1+2+3}$ and clinical outcome, we estimated $IIP_{ave1+2+3}$ more precisely using a weighted average of the relevant pairwise DI values (**Fig. 4** and **Supplementary Table 6**). By accounting for different modes of pairwise interaction, this approach gives better agreement with experimentally determined $IIP_{ave1+2+3}$ than either the Loewe or Bliss models (**Supplementary Fig. 5** and **Supplementary Table 7**). Despite the complicating factor of regimen tolerability, predictions of $IIP_{ave1+2+3}$ based on DI index values correlated well with clinical outcome (**Supplementary Fig. 6**, correlation coefficient = 0.686, $P < 0.001$). Only 1 of 31 evaluated regimens with $IIP_{ave1+2+3} < 8$ had >70% of subjects with a viral load <50 copies per ml at 48 weeks. Among evaluated regimens meeting this criterion, the one with the lowest $IIP_{ave1+2+3}$ was TDF plus FTC plus RAL[37]. Using DI values, we estimate an $IIP_{ave1+2+3}$ of 5.05 for this regimen. This is at the high end of the Loewe-Bliss range owing to favorable RAL interactions (**Fig. 4b**). These results suggest that a minimum of 5–8 logs of inhibition are required for successful HAART. The triple NRTI regimen TDF plus 3TC plus ABC had a similar Loewe-Bliss range but inferior efficacy[38], possibly because the actual $IIP_{ave1+2+3}$ value is closer to the low end of the Loewe-Bliss range (because of low DI for ABC pairs) and below the 5-log threshold (**Fig. 4b**). Three of the other regimens currently recommended for initial treatment had $IIP_{ave1+2+3} > 8$, primarily owing to the IIP of the base drug (EFV, ATV/r, DRV/r) . Above $IIP_{ave1+2+3} = 7$, there was little correlation with outcome (correlation coefficient = 0.125, $P = 0.29$) because above this level, replication is essentially halted, and outcome depends mainly on adherence.

This approach provides a quantitative basis for HAART. HAART controls viral replication because of steep, upwardly inflected dose-response curves for some drugs and synergies reflecting the independent action for other drugs. Despite the extremely high IIP_{ave} of some regimens, HAART is not curative because of stable reservoirs of nonreplicating virus[39,40]. Our results demarcate a minimum threshold level of antiviral activity (IIP_{ave} = 5–8 logs) necessary for successful treatment. Above this range, additional inhibitory potential is not necessarily beneficial, particularly if it involves the use of poorly tolerated drugs. Evaluating new regimens in relation to this threshold may reduce the need for costly clinical trials for regimens lacking sufficient IIP_{ave}. This approach also permits a comprehensive search for regimens with suprathreshold antiviral activity, maximum tolerability and minimum cost. Simpler two- or three-drug regimens with adequate IIP_{ave} but lower cost and toxicity may be important for extending therapy in resource-limited settings. Finally, this approach may allow more rational selection of salvage regimens.

METHODS

Methods and any associated references are available in the online version of the paper at http://www.nature.com/naturemedicine/.

Note: Supplementary information is available on the Nature Medicine website.

ACKNOWLEDGMENTS

We thank J. Blankson, A. Spivak, C. Durand, J. Gallant, J. Cofrancesco and W. Greco for helpful discussions. This work was supported by US National Institutes of Health grant AI081600 and by the Howard Hughes Medical Institute.

AUTHOR CONTRIBUTIONS

B.L.J., M.Z., M.E.S., C.K.B. and J.L. conducted the experiments. B.L.J., M.Z., S.A.R., L.S. and R.F.S. carried out the computational analysis. R.F.S. supervised the project and wrote the manuscript.

COMPETING FINANCIAL INTERESTS

The authors declare no competing financial interests.

Published online at http://www.nature.com/naturemedicine/.
Reprints and permissions information is available online at http://www.nature.com/reprints/index.html.

1. Gulick, R.M. *et al.* Treatment with indinavir, zidovudine, and lamivudine in adults with human immunodeficiency virus infection and prior antiretroviral therapy. *N. Engl. J. Med.* **337**, 734–739 (1997).
2. Hammer, S.M. *et al.* A controlled trial of two nucleoside analogues plus indinavir in persons with human immunodeficiency virus infection and CD4 cell counts of 200 per cubic millimeter or less. AIDS Clinical Trials Group 320 Study Team. *N. Engl. J. Med.* **337**, 725–733 (1997).

3. Perelson, A.S. *et al.* Decay characteristics of HIV-1-infected compartments during combination therapy. *Nature* **387**, 188–191 (1997).
4. Walensky, R.P. *et al.* The survival benefits of AIDS treatment in the United States. *J. Infect. Dis.* **194**, 11–19 (2006).
5. Wei, X. *et al.* Viral dynamics in human immunodeficiency virus type 1 infection. *Nature* **373**, 117–122 (1995).
6. Ho, D.D. *et al.* Rapid turnover of plasma virions and CD4 lymphocytes in HIV-1 infection. *Nature* **373**, 123–126 (1995).
7. Coffin, J.M. HIV population dynamics *in vivo*: implications for genetic variation, pathogenesis, and therapy. *Science* **267**, 483–489 (1995).
8. Perelson, A.S., Neumann, A.U., Markowitz, M., Leonard, J.M. & Ho, D.D. HIV-1 dynamics in vivo: virion clearance rate, infected cell life-span and viral generation time. *Science* **271**, 1582–1586 (1996).
9. Wodarz, D. & Nowak, M.A. Mathematical models of HIV pathogenesis and treatment. *Bioessays* **24**, 1178–1187 (2002).
10. Thompson, M.A. *et al.* Antiretroviral treatment of adult HIV infection: 2010 recommendations of the International AIDS Society-USA panel. *J. Am. Med. Assoc.* **304**, 321–333 (2010).
11. Department of Health and Human Services Panel on Antiretroviral Guidelines for Adults and Adolescents. Guidelines for the use of antiretroviral agents in HIV-1–infected adults and adolescents. 〈http://www.aidsinfo.nih.gov/ContentFiles/AdultandAdolescentGL.pdf〉 (2009).
12. Shen, L. *et al.* Dose-response curve slope sets class-specific limits on inhibitory potential of anti-HIV drugs. *Nat. Med.* **14**, 762–766 (2008).
13. Hill, A.V. The possible effects of the aggregation of the molecules of huemoglobin on its dissociation curves. *J. Physiol. (Lond.)* **40**, 4–7 (1910).
14. Chou, T.C. Derivation and properties of Michaelis-Menten type and Hill type equations for reference ligands. *J. Theor. Biol.* **59**, 253–276 (1976).
15. Holford, N.H. & Sheiner, L.B. Understanding the dose-effect relationship: clinical application of pharmacokinetic-pharmacodynamic models. *Clin. Pharmacokinet.* **6**, 429–453 (1981).
16. Greco, W.R., Bravo, G. & Parsons, J.C. The search for synergy: a critical review from a response surface perspective. *Pharmacol. Rev.* **47**, 331–385 (1995).
17. Chou, T.C. Theoretical basis, experimental design, and computerized simulation of synergism and antagonism in drug combination studies. *Pharmacol. Rev.* **58**, 621–681 (2006).
18. Sampah, M.E., Shen, L., Jilek, B.L. & Siliciano, R.F. Dose-response curve slope is a missing dimension in the analysis of HIV-1 drug resistance. *Proc. Natl. Acad. Sci. USA* **108**, 7613–7618 (2011).
19. Ferguson, N.M., Fraser, C. & Anderson, R.M. Viral dynamics and anti-viral pharmacodynamics: rethinking in vitro measures of drug potency. *Trends Pharmacol. Sci.* **22**, 97–100 (2001).
20. Chou, T.C. & Talalay, P. Quantitative analysis of dose-effect relationships: the combined effects of multiple drugs or enzyme inhibitors. *Adv. Enzyme Regul.* **22**, 27–55 (1984).
21. Shen, L. *et al.* A critical subset model provides a conceptual basis for the high antiviral activity of major HIV drugs. *Sci. Transl. Med.* **3**, 91ra63 (2011).
22. Walmsley, S. *et al.* Lopinavir-ritonavir versus nelfinavir for the initial treatment of HIV infection. *N. Engl. J. Med.* **346**, 2039–2046 (2002).
23. Siliciano, J.D. & Siliciano, R.F. Biomarkers of HIV replication. *Curr. Opin. HIV. AIDS* **5**, 491–497 (2010).
24. Katlama, C. *et al.* Efficacy of darunavir/ritonavir maintenance monotherapy in patients with HIV-1 viral suppression: a randomized open-label, noninferiority trial, MONOI-ANRS 136. *AIDS* **24**, 2365–2374 (2010).
25. Peréz-Valero, I. & Arribas, J.R. Protease inhibitor monotherapy. *Curr. Opin. Infect. Dis.* **24**, 7–11 (2011).
26. Bierman, W.F., van Agtmael, M.A., Nijhuis, M., Danner, S.A. & Boucher, C.A. HIV monotherapy with ritonavir-boosted protease inhibitors: a systematic review. *AIDS* **23**, 279–291 (2009).
27. Markowitz, M. *et al.* Rapid and durable antiretroviral effect of the HIV-1 Integrase inhibitor raltegravir as part of combination therapy in treatment-naive patients with HIV-1 infection: results of a 48-week controlled study. *J. Acquir. Immune Defic. Syndr.* **46**, 125–133 (2007).
28. Cooper, D.A. *et al.* Maraviroc versus efavirenz, both in combination with zidovudine-lamivudine, for the treatment of antiretroviral-naive subjects with CCR5-tropic HIV-1 infection. *J. Infect. Dis.* **201**, 803–813 (2010).
29. Bliss, C.I. The toxicity of poisons jointly applied. *Ann. Appl. Biol.* **26**, 585–615 (1939).
30. Loewe, S. & Muischnek, H. Effect of combinations: mathematical basis of problem. *Arch. Exp. Pathol. Pharmakol.* **114**, 313–326 (1926).
31. Kohlstaedt, L.A., Wang, J., Friedman, J.M., Rice, P.A. & Steitz, T.A. Crystal structure at 3.5 A resolution of HIV-1 reverse transcriptase complexed with an inhibitor. *Science* **256**, 1783–1790 (1992).
32. Hoggard, P.G., Kewn, S., Barry, M.G., Khoo, S.H. & Back, D.J. Effects of drugs on 2′,3′-dideoxy-2′,3′-didehydrothymidine phosphorylation in vitro. *Antimicrob. Agents Chemother.* **41**, 1231–1236 (1997).
33. Havlir, D.V. *et al. In vivo* antagonism with zidovudine plus stavudine combination therapy. *J. Infect. Dis.* **182**, 321–325 (2000).
34. Wyma, D.J. *et al.* Coupling of human immunodeficiency virus type 1 fusion to virion maturation: a novel role of the gp41 cytoplasmic tail. *J. Virol.* **78**, 3429–3435 (2004).
35. Murakami, T., Ablan, S., Freed, E.O. & Tanaka, Y. Regulation of human immunodeficiency virus type 1 Env-mediated membrane fusion by viral protease activity. *J. Virol.* **78**, 1026–1031 (2004).
36. Müller, B. *et al.* HIV-1 Gag processing intermediates trans-dominantly interfere with HIV-1 infectivity. *J. Biol. Chem.* **284**, 29692–29703 (2009).
37. Lennox, J.L. *et al.* Safety and efficacy of raltegravir-based versus efavirenz-based combination therapy in treatment-naive patients with HIV-1 infection: a multicentre, double-blind randomised controlled trial. *Lancet* **374**, 796–806 (2009).
38. Gallant, J.E. *et al.* Early virologic nonresponse to tenofovir, abacavir, and lamivudine in HIV-infected antiretroviral-naive subjects. *J. Infect. Dis.* **192**, 1921–1930 (2005).
39. Finzi, D. *et al.* Identification of a reservoir for HIV-1 in patients on highly active antiretroviral therapy. *Science* **278**, 1295–1300 (1997).
40. Finzi, D. *et al.* Latent infection of CD4+ T cells provides a mechanism for lifelong persistence of HIV-1, even in patients on effective combination therapy. *Nat. Med.* **5**, 512–517 (1999).

ONLINE METHODS

We measured drug inhibition of HIV-1 infection using a single-round infectivity assay as previously described[12,18]. We chose a single-round assay because complex factors such as growth and death of target cells distort *m* in multiround assays[19]. To accurately mimic infection events *in vivo*, we carried out infections in primary $CD4^+$ T lymphoblasts obtained by phytohemagglutinin (Remel, Leneva) activation of peripheral blood mononuclear cells from healthy donors as previously described[18]. All blood donors provided informed consent according to a protocol approved by the Johns Hopkins Institutional Review Board. We infected $CD4^+$ T lymphoblasts with recombinant HIV-1 pseudoviruses generated by transfection of HEK293 T cells (American Type Culture Collection) with a previously described[12] HIV-1 vector (pNL43-ΔE-EGFP) containing a GFP-tagged defective envelope. The envelope was provided in *trans* by co-transfection with an envelope expression vector. In most cases, we used a CXCR4-tropic envelope (HXB2; NIH AIDS Research and Reference Reagent Program) because it gave higher-level infection of primary $CD4^+$ T lymphoblasts, thus affording a wider dynamic range. However, IC_{50}' and m' values obtained in infections with CCR5-tropic pseudoviruses were not significantly different from those obtained with CXCR4-tropic viruses (**Supplementary Table 8**), and modes of drug interaction were also similar (**Supplementary Table 7**). To account for individual variation in cellular uptake and metabolism of drugs, we performed replicate assays in lymphoblasts from 10–60 healthy donors for each drug and computed average levels of inhibition. We used high serum concentrations (55%) to account for protein binding. For protein-bound drugs, titrations of drug effect versus serum concentration demonstrated that inclusion of 50% human serum and 5% FCS provided a close approximation for *in vivo* drug binding. We pre-tested lots of human serum for low toxicity to $CD4^+$ T lymphoblasts. Drugs were added to lymphoblast targets, and cells were incubated at 37 °C for 16 h before infection to allow sufficient time for triphosphorylation of NRTIs. Longer preincubations did not enhance antiviral activity. Protease inhibitors were also added at the stage of virus production in 293T cells[18]. After spin infection in 96 well plates, targets were incubated for 3 days at 37 °C. Cells were then fixed in 2% formaldehyde, and GFP expression was analyzed by flow cytometry. After gating for viable cells, the fraction of infection events unaffected by drug (f_u) was determined as the % GFP^+ cells in the presence of drug divided by the % GFP^+ cells in control wells without drug. Calculation of IIP from f_u is described in the **Supplementary Methods**. All drugs were obtained from the NIH AIDS Research and Reference Reagent Program.

To determine whether the combined effect of two antiretroviral drugs followed the predictions of the Bliss or Loewe models, we tested pairs of drugs at constant molar ratios chosen to maximize the difference between the levels of inhibition predicted by the two models. Drug combinations are often evaluated in surface experiments in which all possible combinations of several different concentrations of each drug are tested[26,27]. However, the difference between the inhibition predicted by the two models increases with drug concentration (**Fig. 2b**) and is maximal when both drugs contribute equally to the observed suppression (R.F.S., unpublished observation). Therefore, we chose drug concentrations such that at the highest concentrations used, the total inhibition predicted by the Bliss model would be within the dynamic range of the assay (IIP < 3), with each drug contributing equally. Drugs were mixed at these concentrations and serially diluted. Experimental analysis was carried out in cells from 5–15 donors per combination as described above. Protease inhibitors were added at the virus production stage. Analysis of combination experiments is described in the **Supplementary Methods**.

Additional methods. Detailed methodology is described in the **Supplementary Methods**.